

DRIFT CHAMBER DEVELOPMENT AT NAL

M. Atac, W. Taylor, and J. Urish

January 1974



DRIFT CHAMBER DEVELOPMENT AT NAL
M. Atac, W. Taylor and J. Urish
National Accelerator Laboratory
Batavia, Illinois

ABSTRACT

A drift chamber of 1 cm drift spacing with an electric field shaping network has been built, and a computer program was developed for determining the field shaping voltages around the signal wire to obtain uniform electron drift velocities. Several gas mixtures have been studied using this chamber to determine space to drift-time linearity with cosmic rays. The results show that spatial resolutions of 100-150 microns can be obtained from a single chamber operating at atmospheric pressure.

INTRODUCTION

The position of charged particle tracks in space can be measured from the drift time of primary electrons in wire chambers.¹ A CERN-Heidelberg group (1973) used this technique to determine the branching ratio $K^+ \rightarrow e^+ \nu / K^+ \rightarrow \mu^+ \nu$.² There has been increasing interest in drift chamber development by experimenters such as F. Sauli (CERN), J. Saudinos (Orsay), and C. Rubbia (Harvard) in the last two years.

This type of detector is rather attractive for high energy particle detection for the following reasons:

1. Spatial Resolution. Spatial resolution obtained from drift chambers varies from 0.15 mm to 1.25 mm for drift spacings on the order of 2.4 cm to 50.0 cm.^{3,4} It has been demonstrated that 0.35 mm resolution can be obtained across an area of $4 \times 4 \text{ m}^2$ with a 5 cm drift distance.⁵ Obtaining a resolution better than 0.5 mm from multiwire proportional chambers, operated at atmospheric pressure, which are larger than $10 \times 10 \text{ cm}^2$ in area is difficult.⁶

2. Time Resolution. Using the same wire, two simultaneous tracks, which are separated by at least 50 nsec in drift time, are capable of being resolved.

3. Multiple Track Resolution. Two simultaneous tracks, which are separated by 2.5 mm, can be distinguished.

4. Rate Capability. Drift chambers with count rates of 10^5 particles per second per cm of signal wire are possible.

5. Construction. Drift chambers are relatively simple to construct compared to other detectors offering similar resolution.

CONSTRUCTION

Figure 1 is a cross-sectional view of the drift chamber region which contains three separate signal wires (12 micron diameter) alternating between high-voltage field shaping wires

(100 micron diameter). The signal wires are stretched between two parallel wire planes along which the voltage was applied to maintain uniform field conditions in the drift region. The desired voltage pattern on the plane was supplied from a resistive voltage divider circuit shown in Figure 2. The entire assembly was constructed on a standard G-10 frame giving an active drift area of about 6 x 15 cm². The detector network itself was then mounted inside a 30 cm x 33 cm chamber which can be pressurized up to four atmospheres. The active area of the detector was positioned between two 35 micron thick stainless steel windows (15 cm diameter).

The drift time is measured by a time to amplitude converter (TAC) and stored in a multichannel analyzer (see Figure 3). A coincidence pulse obtained from the plastic scintillators starts the TAC and the pulse from the drift chamber stops it. The plastic scintillators were large enough (15 x 15 cm²) to cover the entire sensitive area of the drift chamber. The amplifier circuit, designed by C. Kerns, has an input threshold sensitivity of 0.5 mV across a 500Ω input resistor.

FIELD PLOTS

Equipotential surfaces in the chamber indicated in Figure 1 were calculated by computer from the known voltages V_i on the field shaping wires. The technique was to solve the set of linear equations

$$V_i = \sum_j \lambda_j \ln (d_j/x_{ij}) \quad (\text{adjusted units}) \quad (1)$$

for the charge densities λ_j , where the distance from a signal wire at ground potential to the j^{th} wire is d_j which was separated from the i^{th} wire by x_{ij} . The indices in Equation 1 include all wires in the drift chamber, and when $i = j$ then x_{ij} would be the radius of the wire. In addition, the sum of the charge densities on the high voltage wires must equal the charge density on the signal wires. Once the λ_j are determined, Equation 1 may be again used to compute the potential at any point in the drift region of the chamber. Two criteria in the computer design for an optimal voltage combination

were to produce nearly concentric equipotentials and maintain a uniform field in the drift space. Concentric equipotentials reduce ambiguities caused by large-angle particle trajectories through the chamber and at the same time eliminate dead regions where electrons can become delayed. For comparison, the equipotential surfaces in the drift region were plotted on special resistive paper (teledeltos) that was scaled to the dimensions of the chamber using the computed field shaping voltages. These techniques are in good agreement as seen in Figure 1.

Further development of drift chamber configurations is being continued since the drift velocity of electrons in the gas mixture, which is determined by the electric field intensity, affects the space-time linearity of the chamber.

DATA

The spectrum of events in the chamber obtained from the drift time of the electrons can be displayed in terms of the position of the ionizing particle that causes an event. This is automatic if the time to distance relationship can be made linear. If we assume that cosmic rays would enter the active area of the chamber in a random manner (angular corrections were determined to be below statistics) so as to produce a uniform spatial distribution of events, then the space coordinates x_j of the distribution are related to the drift time t_i by the equation

$$x_j = a \frac{\sum_{i=1}^j f(t_i)}{N \sum_{i=1} f(t_i)} \quad (2)$$

The total drift distance $a = 1$ cm corresponds to the total drift time produced by N channels in the time spectrum $f(t_i)$ obtained from the multichannel analyzer. We see observable nonlinearities in the space-time relations from the Figures 4, 5, 6, and 7 with 17% C_2H_2 + 83% Ar, 10% CH_4 + 90% Ar, 80% C_2H_4 + 20% Ar, and 30% $i-C_4H_{10}$ + 70% Ar gas mixtures respectively. At high field regions the drift velocity is decreased in the Methane-Argon mixture and it is increased in the Acetylene-Argon mixture.

Therefore a very linear space-time relation was achieved in Figure 8 when the properties of these two gases were combined using 9.2% CH₄ + 7.5% C₂H₂ + 83% Ar mixture. Each figure contains a photograph of the spectrum taken from the multi-channel analyzer for each gas mixture showing the number of events as a function of drift time. In each case the total high voltage (HV) was varied to obtain optimum operating conditions.

We conclude from this result that the spatial resolution was limited by the accuracy of the readout electronics. Time slewing due to the fixed threshold discrimination in the amplifier-discriminator circuit is minimal (less than 2 nanoseconds) due to the fast-rising large pulses. The rise time of the pulses obtained from the Argon-Methane-Acetylene mixture was less than 8 nanoseconds. It is quite feasible to provide ± 2 nsec timing using present day electronics for the readout system.⁷ Thus a spatial resolution of 100 micron is quite obtainable from drift chambers with a field shaping network using this gas mixture.

ACKNOWLEDGMENTS

The authors would like to express their thanks to C. Kerns for the amplifier circuit and S. Cepeda for his assistance in the field plots.

REFERENCES

1. G. Charpak, et. al., Nucl. Instr. & Meth. 62(1968)282.
2. A. H. Walenta, Nucl. Instr. & Meth. 111(1973)467-475.
3. F. Sauli, Drift Chamber Conference, Nov. 14- 1973 (to be published).
4. J. Saudinos, Proceedings of 1973 International Conference on Instrumentation for High Energy Physics, pp. 316.
5. C. Rubbia, et. al., Proceedings of 1973 International Conference on Instrumentation for High Energy Physics, pp. 268.

6. M. Atac, IEEE Transactions on Nuclear Science, Vol. NS-19, No. 3(1972)144.
7. E. Schüller, CERN NP Internal Report 73-15, Sept. 28, 1973.

FIGURE CAPTIONS

- Figure 1. A cross-sectional view of the drift chamber region showing the equipotential surfaces around the signal wire plotted from teledeltos paper (top) and by computer (bottom).
- Figure 2. The resistive voltage divider circuit producing the field shaping voltages for the entire drift chamber. The bottom view shows the alternate signal wires.
- Figure 3. Electronics logic for the drift chamber detector.
- Figure 4. Acetylene-Argon mixture. The space-time relation obtained from the time spectrum indicates that the drift velocity increases for higher electric fields as the electrons approach the multiplication region.
- Figure 5. Methane-Argon mixture. The space-time relation obtained from the time spectrum indicates that the drift velocity decreases for higher electric fields as the electrons approach the multiplication region.
- Figure 6. Ethelyne-Argon mixture. A nonlinearity occurs for both the low and high field regions as is indicated by the continual decreasing of events in the time spectrum.

Figure 7. Argon-Isobutane mixture. The space-time linearity obtained from the time spectrum is fair with the exception of the observed saturation in the multiplication region.

Figure 8. Argon-Methane-Acetylene mixture. The opposing properties of methane and acetylene were combined to yield a very linear space-time relation as seen in the randomness of events in the time spectrum.

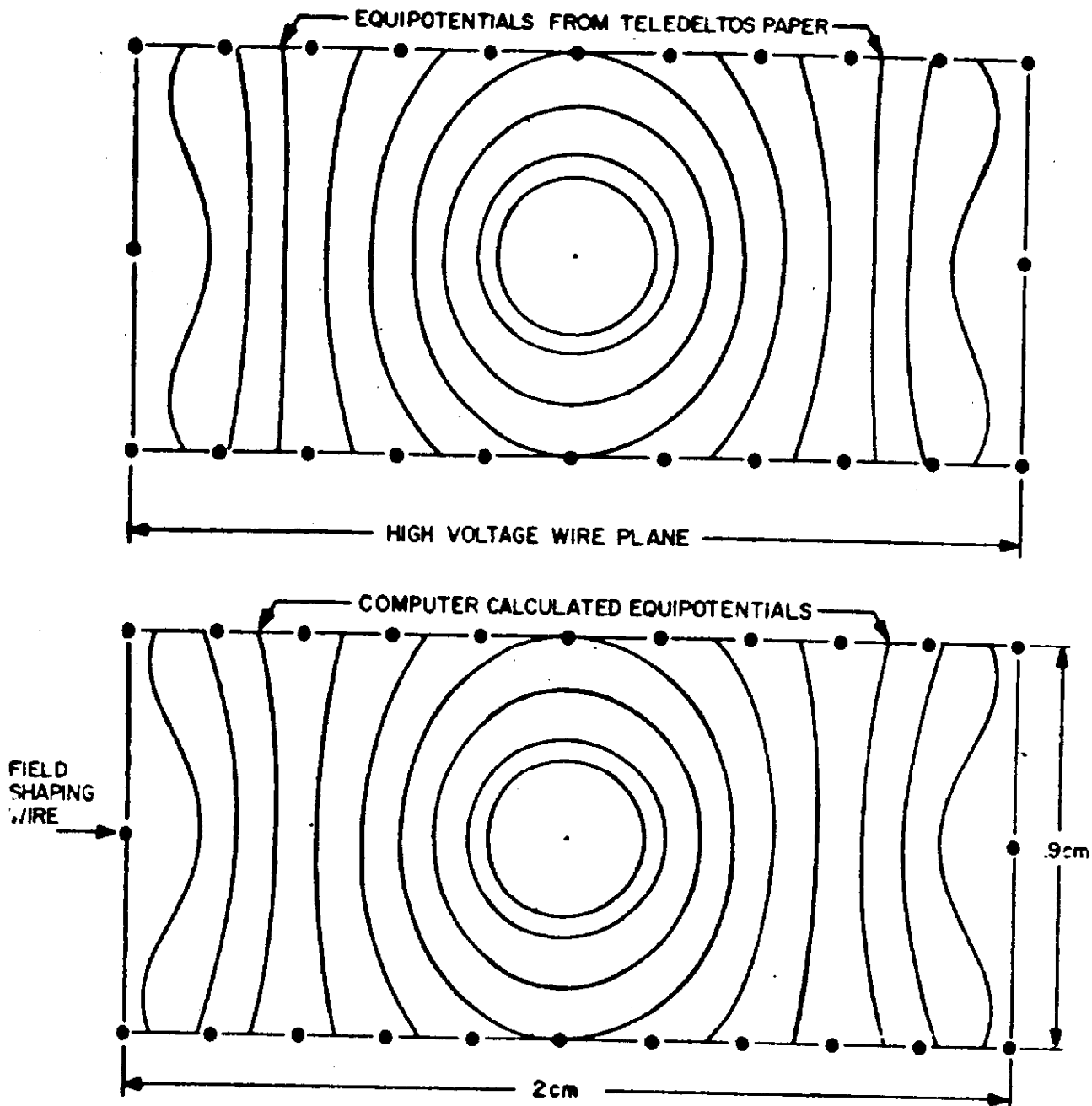


Fig. 1

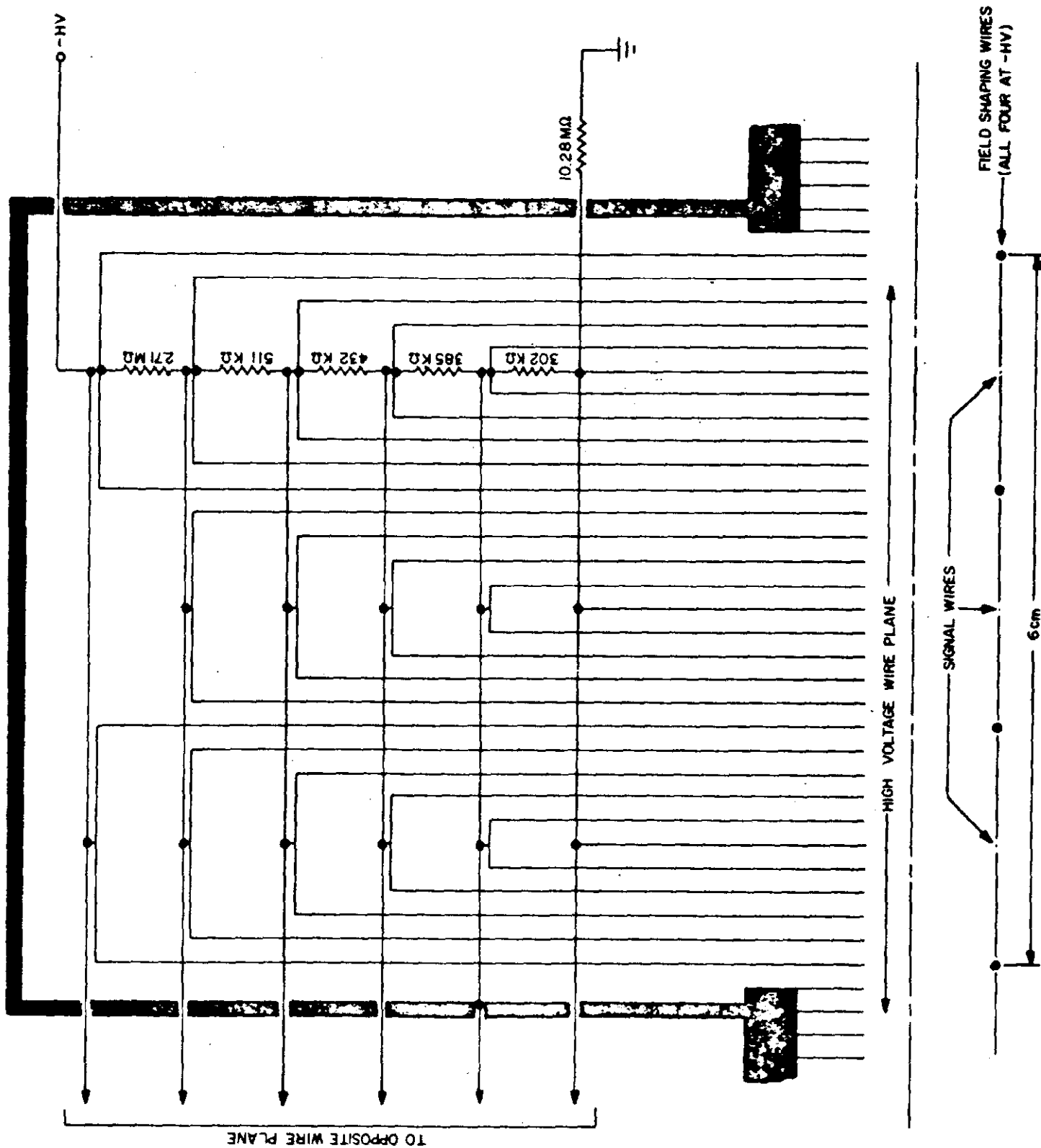


Fig. 2

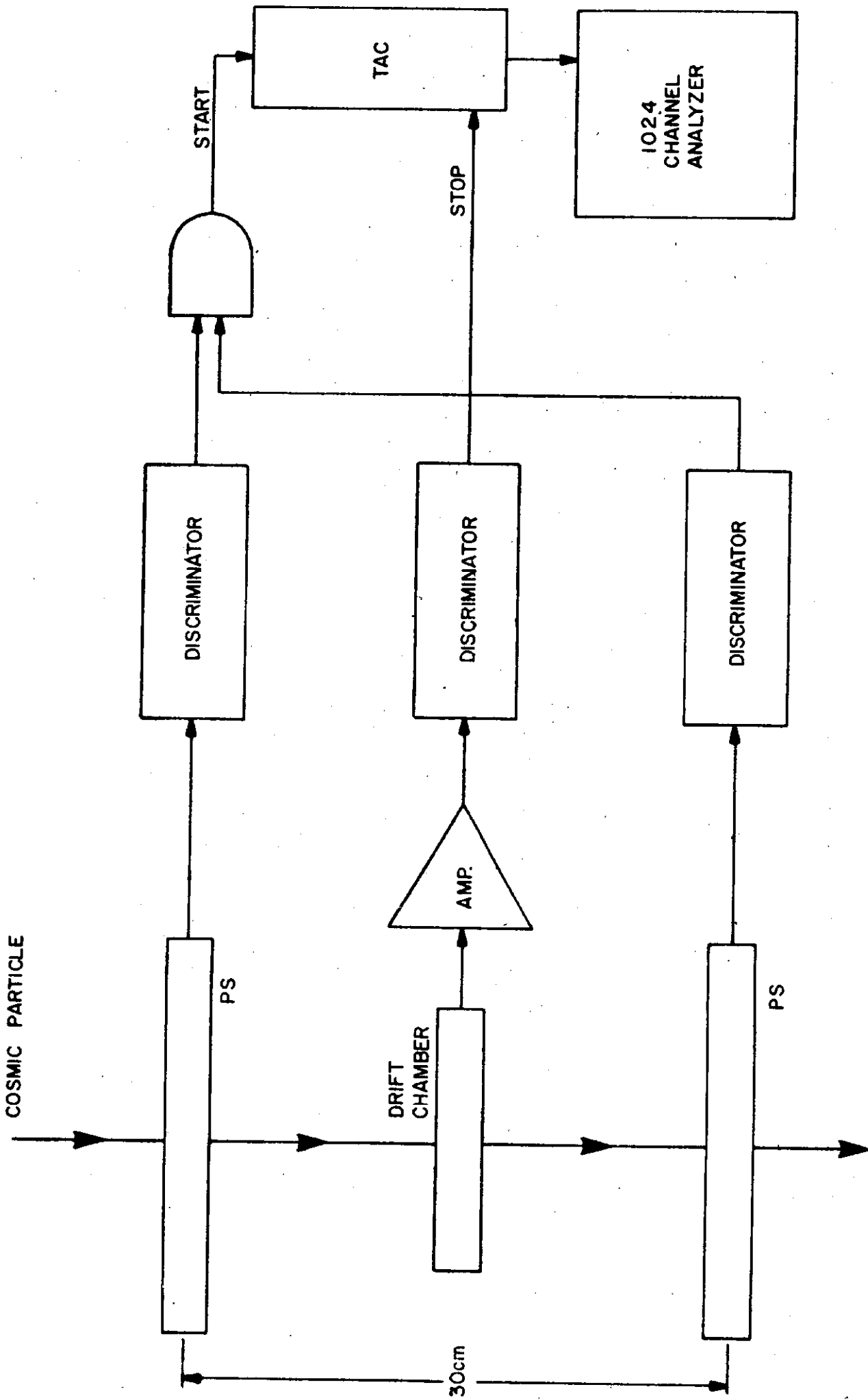


Fig.3

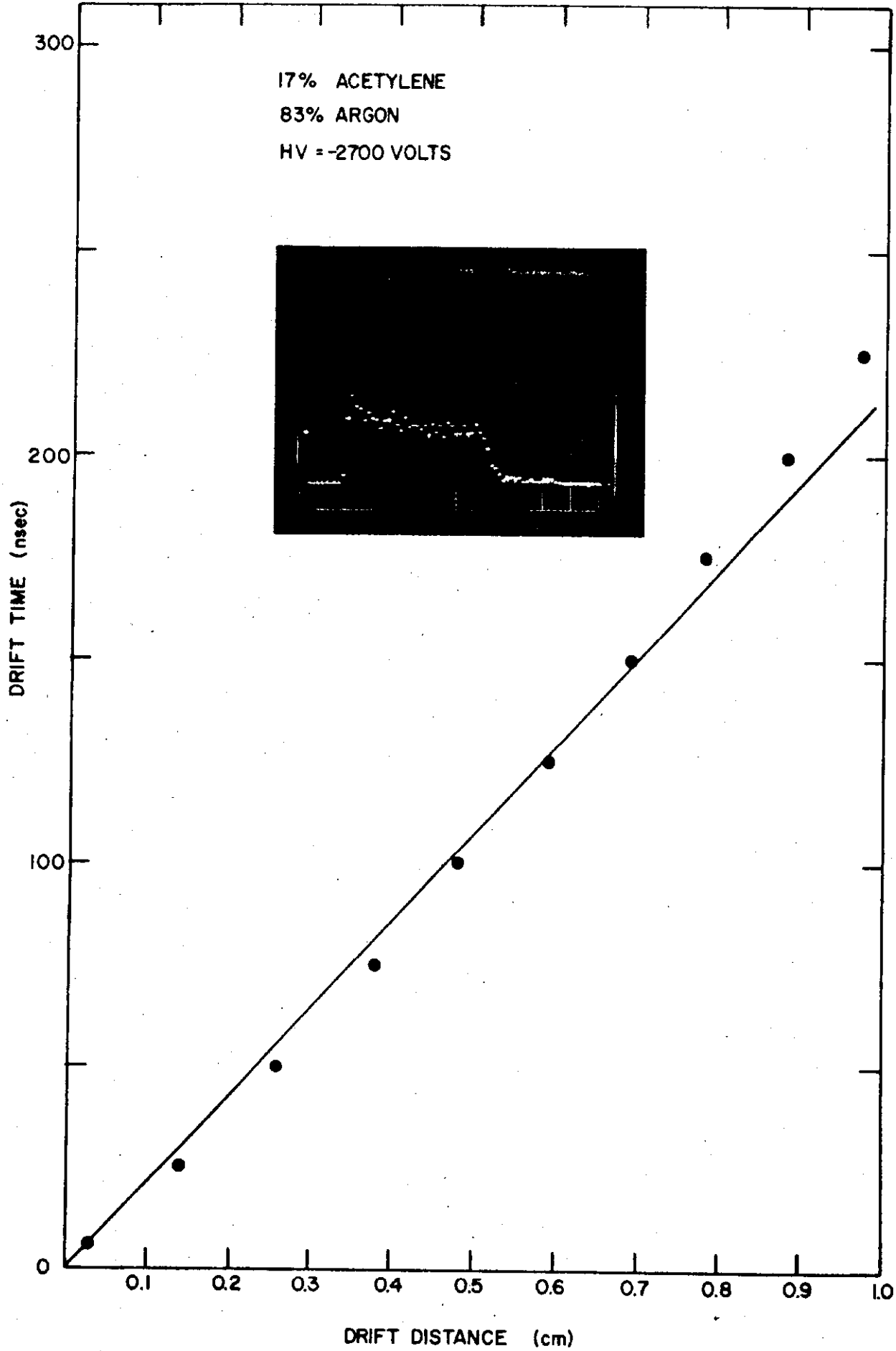


Fig. 4

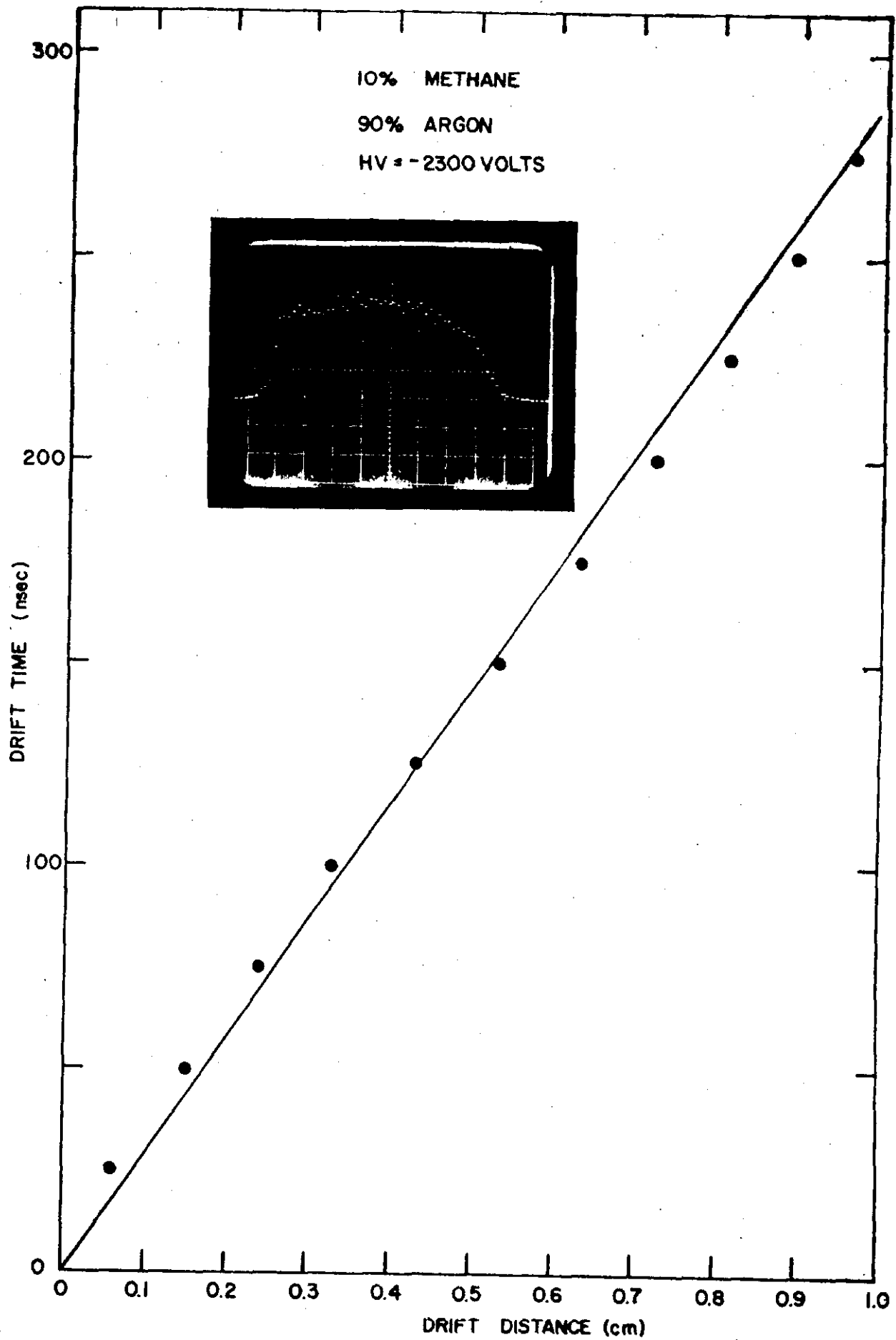


Fig. 5

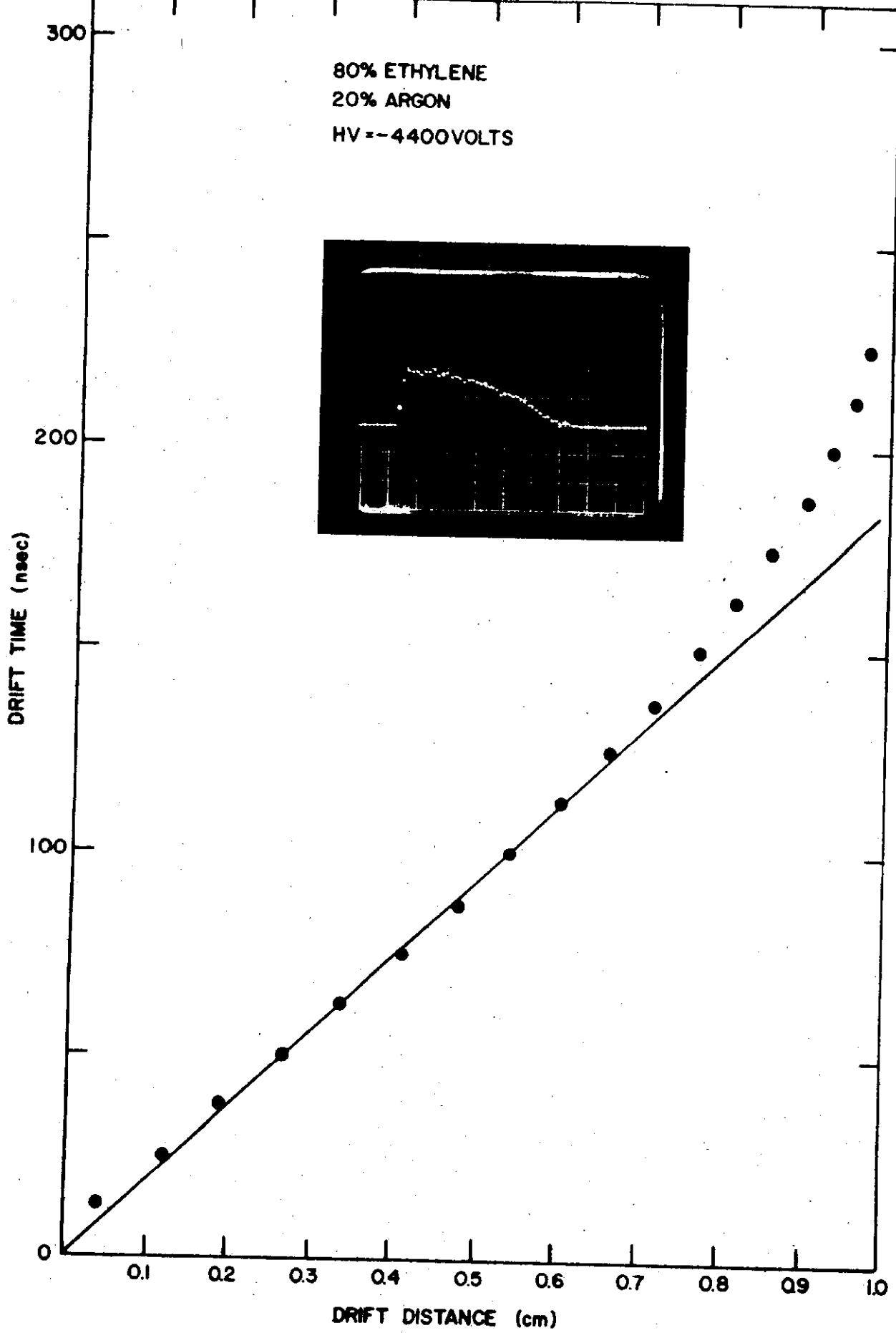


Fig.6

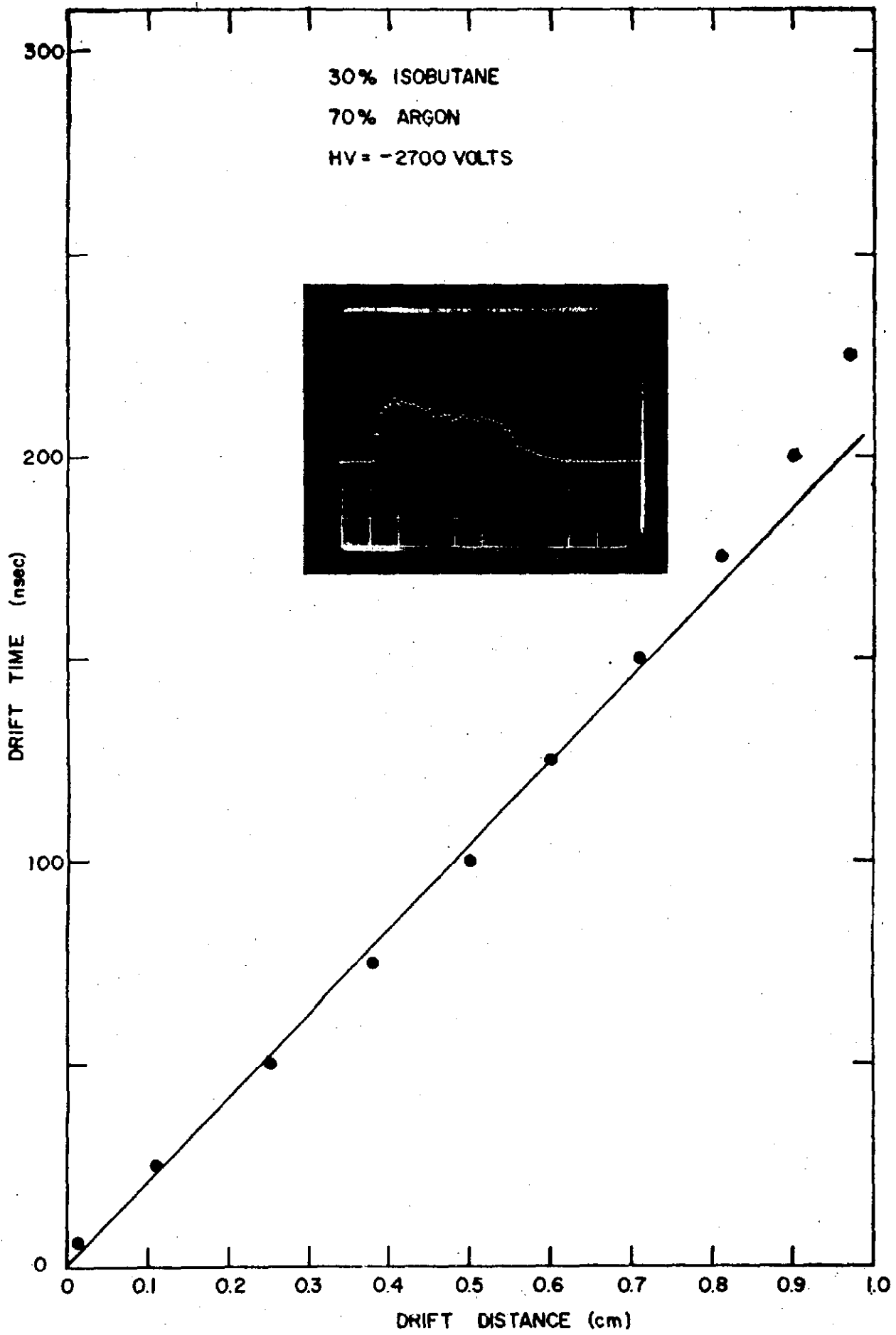


Fig.7

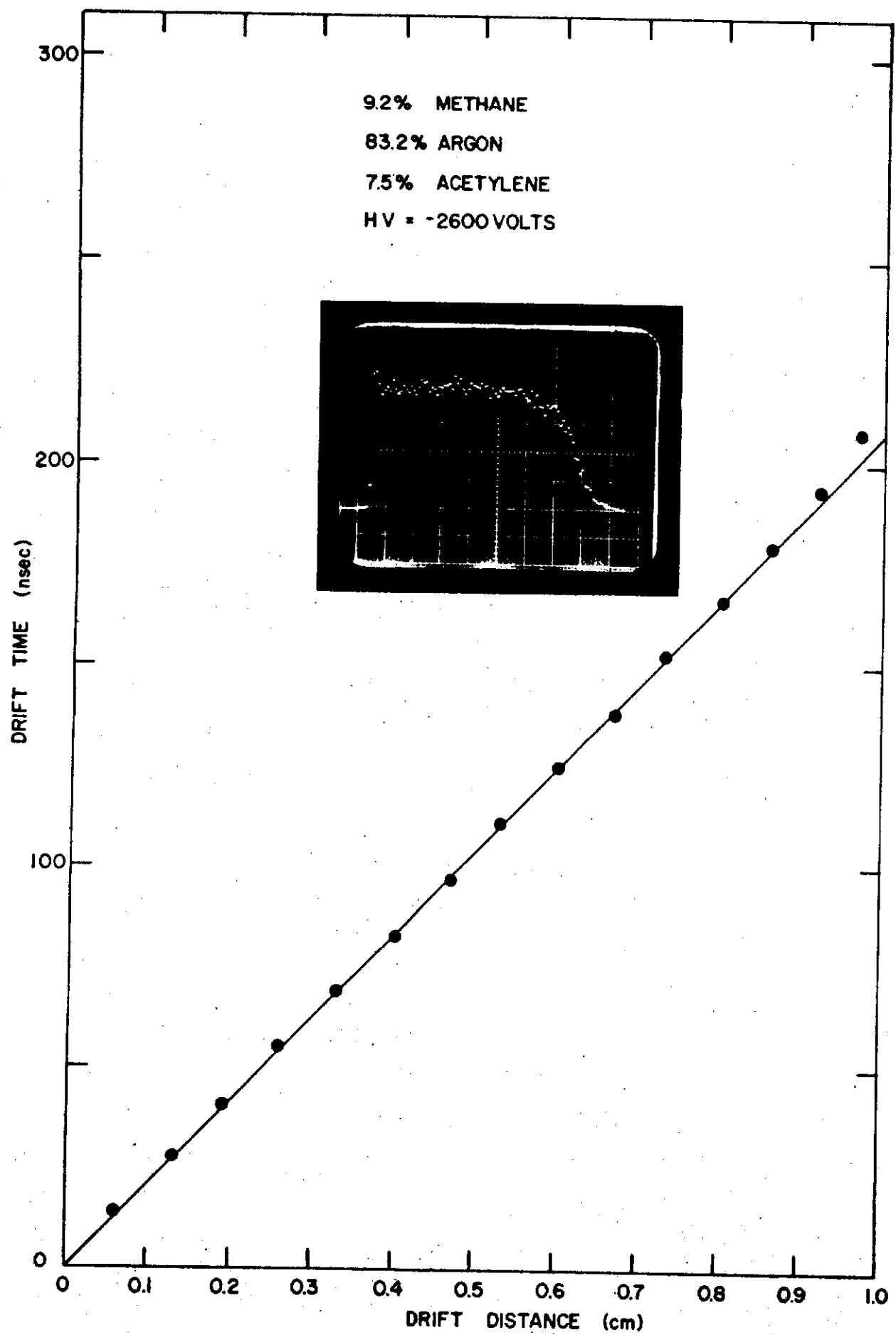


Fig.8